PORT AND OCEAN ENGINEERING UNDER ARCTIC CONDITIONS
TECHNICAL UNIVERSITY OF NORWAY

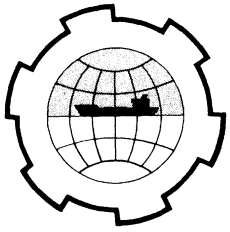

PRESSURE RIDGE CHARACTERISTICS IN THE ARCTIC COASTAL ENVIRONMENT

W.F. Weeks
A. Kovacs
W.D. Hibler, III

U.S. Army Cold Regions Research and Engineering Laboratory — Hanover, New Hampshire USA

ABSTRACT

The Arctic ice pack is characterized by extreme irregularities in ice thickness which are produced by the motion and resulting deformation of the sea ice. Pressure ridges and hummocks, which are the largest of the ice relief features, present formidable problems to both the design of off-shore facilities and to the operation of surface and subsurface shipping. The mechanics of ridge and hummock formation are reviewed and it is shown that several distinct types of ice deformation features occur depending upon whether the formation mechanism is marginal crushing, overthrusting or shearing.

Between 1969 and the present a number of both free-floating and grounded ridges have been examined by the authors in the Bering, Chukchi and Beaufort Seas. Profiles of the upper and lower surfaces of the ridges were determined by leveling and by drilling and sonar, respectively, and the internal structure of the ridges was investigated by coring. Ice temperatures, salinities, and densities were obtained and brine volumes were computed from the temperatures and salinities. Representative profiles are presented. The present results of this program are:

1. The degree of bonding between ice blocks and, therefore, the overall structural integrity of ridge keels would appear to be variable, presumably changing with the age of the ridge and the initial temperature of the ice being incorporated into the ridge. It can be shown that during the winter the cold reserve of ice blocks being incorporated into a ridge can be sufficient to cause significant inter-block ice growth.

2. Lack of local isostatic adjustment is common in ridges. A significant portion of the ridge load is apparently supported by the surrounding ice resulting in its deflection. When ridges form by thrusting, their upper and lower portions may be laterally separated by tens of meters. This obviously results in a non-isostatic condition which is compensated by deflections of the local plate ice.

3. A representative salinity for the ice in the ridges we examined was $4^0/_{00}$ for first-year ridges and $3^0/_{00}$ for multi-year ridges. The temperature profiles were reasonably linear except in the lower parts of ridges with pronounced keels where temperatures were roughly constant at near freezing values.

4. Present information indicates that the average surface slope angle of the above-water portion of a first-year ridge (24°) is less than that of the subsurface slope (33°). The average surface slope angle of the one multi-year ridge studied was 19°.

5. Multi-year ridges were found to be massive in size and "solid" when cored.

6. Ridges act as effective snow fences, causing large amounts of snow to accumulate both in and around their upper parts.

7. It appears doubtful that the cross-section profiles of all ridges can adequately be represented by any one geometric model.

Current data bearing on the general distribution of deformation features in time and space over the Arctic Ocean are also summarized. The data sources include the BIRDSEYE flights, recent special laser profilometer flights, and sonar traces of the lower ice surface. Prime attention is paid to the ridging characteristics in the Coastal and Offshore Sea Ice Provinces where the ice is clearly more highly deformed than the ice in the Central Arctic Basin Province. Winter and summer distributions of both sail heights and keel depths as well as the number of ridges per nautical mile are presented. Power spectra based on both laser and sonar profiles indicate marked periodicities at some spacings on both the surface and subsurface ice profiles. Although the physical reasons for some of these periodicites are understood (Sastrugi) the reason for peaks at distances such as 82.5 m in the bottom profiles is currently unknown. There are also strong indications that ridge orientation in the Coastal Province is not random. A frequency distribution of ridge keels is derived on general statistical grounds and is fitted to 49 sets of observed distributions with excellent agreement. Using this observed distribution, the probability of encountering a ridge with a keel greater than some specified value in a given length of ice pack can be approximated by a Poisson distribution. An encounter probability for keels of different depths as a function of time and the velocity of the pack is obtained. A mean lifeline calculation based upon this encounter probablility is given.

INTRODUCTION

Man has long been denied ease of passage and has been hampered in his efforts to develop the Arctic's natural resources by the highly irregular and formidable sea ice cover. This cover is forever changing in thickness, extent and relief with the seasons and the natural forces acting upon it. With the exception of a very

narrow belt of fast ice which forms in winter near the coast, the ice cover is in continual motion. Drift rates along the irregular paths traveled by the floes vary from 1.2 to 4.0 nm/day. Maximum drift velocities under rarefied ice conditions occasionally reach 20 nm/day for short periods of time (Dunbar and Wittmann 1963).

In a general way the drifting ice cover or pack ice, can be separated into two main ice types: first-year ice with a thickness of roughly 2 m and salinities ranging between 4 and $14^0/_{00}$ and multi-year ice which has survived at least one summer's melt season with a thickness between 2 and 3.5 m and salinities ranging between 0 and $6^0/_{00}$.

That the formation of pressure ridges and hummocked ice are an integral part of the deformation that accompanies ice drift has been known since the earliest days of man's effort to voyage through arctic waters. Detailed observations of ridge formation, properties and distributions have, however, been rare considering that, at the present as in the past, ridges are recognized as the principal impediment to the movement of both surface and subsurface shipping in arctic seas. This paper presents a short review of our current knowledge on this subject.

FORMATION OF RIDGES

Most ridges develop as a result of the deformation of the thinner ice that forms in lead systems between older, thicker floes. Once ridging starts the exact type of ridging will vary with the relative thicknesses of the interacting ice sheets and the nature of the local motion (compression or shear).

If the local motion is primarily compressive, thin ice sheets (less than 20 cm) usually interfinger forming the complex finger-rafting so characteristic when viewed from the air (Fig. 1). For compressive motion in thicker ice a similar interfingering occurs, but the edges of the overthrusts become broken and rounded as a result of the large displacements involved. Each advancing ice sheet pushes its own pile of degris (ice blocks plus snow) ahead of it like a plow (Fig. 2). In many cases we believe that the overthrusting of two interacting ice sheets of equal thickness will cause the sail* of the ridge to be significantly displaced laterally from the keel. Large overthrusts showing a simuous pattern that is grossly similar to finger-rafting are now known to occur in ice more than 2 meters thick (Kovacs, 1971).

If the relative ice motion is compressive and there are appreciable differences in the thicknesses of the two interacting sheets, the thinner sheet will repeatedly fail in bending. This causes a pile of blocks of the thinner ice to

* The upper portions of ridges and hummocks (above the water line) are referred to as sails while the below water portions are called keels.

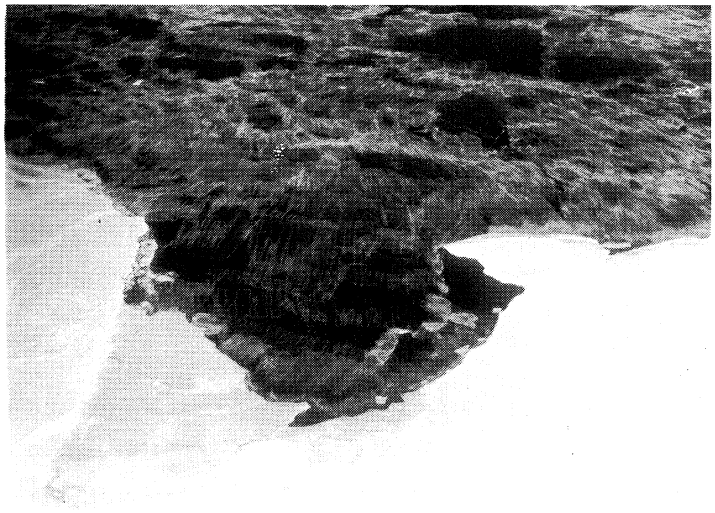

Figure 1. Aerial view of finger-rafting in thin sea ice. Note the tone change in the overthrust produced by the double ice thickness.

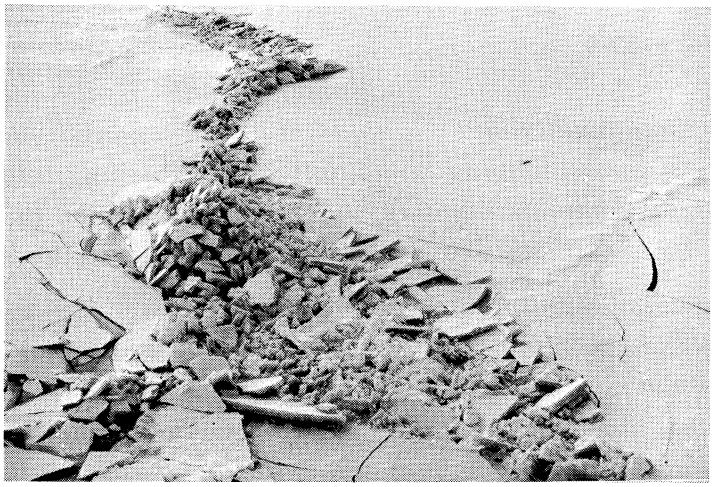

Figure 2. Pressure ridge formation in Viscount Melville Sound. The ice is roughly 0.3 m thick. The ice sheet to the left of the ridge is being thrust over the ice sheet to the right in all but the uppermost portion of the photograph.

accumulate next to the edge of the thicker sheet. As continued failure of the thinner sheet causes the ridge to develop, the general compressive motion will push a portion of the growing ridge onto the upper edge of the thicker ice sheet. Eventually the edge loading of the thicker sheet will cause a segment of it to fail. This segment is then gradually rotated and incorporated into the growing ridge. This process may be repeated a number of times as the ridge grows. Only after the more readily deformed new ice has been pressured into ridges, does ridging involving only the thicker multi-year ice occur. This point was conclusively made by Koerner of the British Trans-Arctic Expedition (personal communica-

tion) who measured the thickness of the slabs in the ridges as he traveled across the Arctic Ocean. Even though 73% of the ice encountered was thick multi-year ice, 81% of the ridges were composed of ice blocks 50 cm or less in thickness. Only 5% of the ridges contained blocks of multi-year ice.

If the relative ice motion is primarily in shear, the resulting ridges are usually very straight in plan view (Fig. 3) allowing them to be differentiated from the air. Shear ridges also characteristically have one near vertical side and many times there is a zone of brecciated ice next to the ridge. The ice in these ridges appear to be completely "ground-up" with only very small fragments of sea ice retaining their identity (Fig. 4). Much of the ice in this type of ridge is compact, granular and featureless suggesting pronounced cataclastic deformation.

Many times the ice deformation does not occur in ridges but as relatively discrete hummocks. In some regions the ice cover may be completely broken up over wide areas forming what might be referred to as a hummocked field (Fig. 5). If there is a significant mechanical difference between the mode of formation of ridges and hummocks, it is not understood. We suspect that isolated hummocks are produced by the crushing of localized pressure points along the irregular initial join between two floes while ridges are produced by more extensive interfloe contact. When this process continues until the ice over an appreciable area has been deformed, a hummocked field is produced.

The highest free-floating ridge we know of was 12.8 m above sea level (Kovacs et al., 1971). As impressive as this ridge was, it is nevertheless a rarety; indeed, ridges in excess of 5 m high are also rare. The deepest keel observed extended some 47 m below sea level (Lyon, personal comments).

It has been shown that the heat sink capacity of the ice blocks incorporated in a ridge keel can be sufficient to freeze the sea water between the blocks (Weeks and Kovacs, 1970a). With time and the effects of ablation, the initially highly irregular block structure of the keel gradually smooths into an undulating surface.

During the melt seasons, the angular ice blocks incorporated in the ridge sail also become rounded, the inter-block voids fill with the refrozen melt of snow and ice and the overall relief becomes rounded (Fig. 6). The number of melt seasons required for a completely rounded relief to develop is related to the location at which the ridge formed and the direction of its drift, i.e., the thermal regime of the environment through which it is moving. For ridges formed in the interior of the Arctic pack, at least two melt seasons are required for the voids between the ice blocks to become filled (Allen Gill, personal comments, 1971). Ridges which survive at least one summer's melt season are referred to as multi-year ridges.

Figure 3. Fragment of a shear ridge north of Barrow, Alaska. Note the vertical side. The ridge height is between 3 and 4 m.

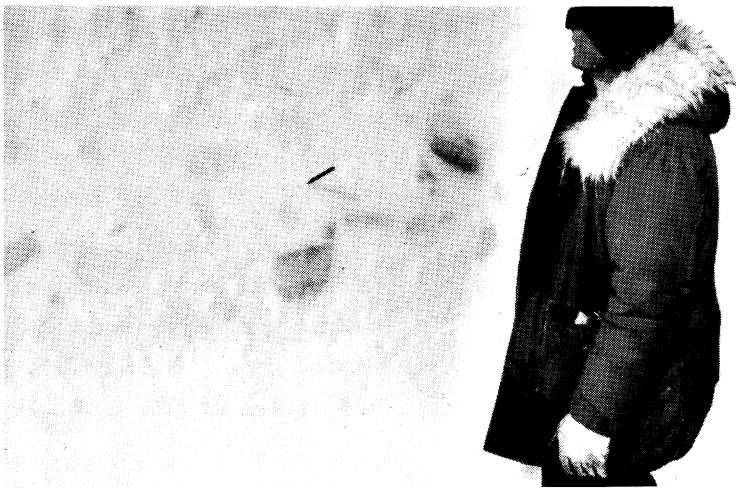

Figure 4. Wall of a shear ridge. With the exception of a few hand-sized fragments, the ridge is composed of massive, granular, fine-grained ice.

Figure 5. A hummock field north of Barrow, Alaska.

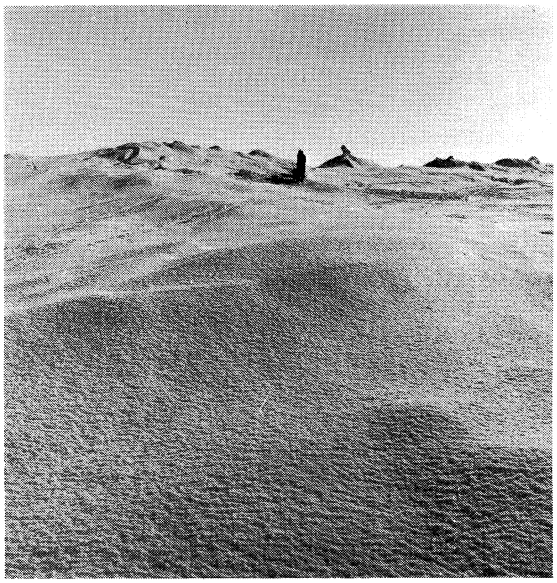

Figure 6. Rounded relief of a multi-year ridge.

PROFILES AND INTERNAL STRUCTURE

In an attempt to gain information on the details of external morphology and the internal structure and physical properties of ridges, a number of representative ridges located in both the fast ice and the pack of the Bering, Chukchi and Beaufort Seas have been examined during the 1969 and 1970 field seasons by CRREL-USCG field parties (Weeks and Kovacs, 1970a and b; Kovacs, 1971; Kovacs, Weeks, Ackley and Hibler, 1971). The profiles of the upper and lower surfaces of the ridges were determined by leveling and by drilling and sonar, respectively, and the centers of the ridges were sampled by coring. Ice temperatures, salinities and densities were measured and brine volumes computed from the temperatures and salinities. As of the present time 13 ridges have been investigated, four of which will be described in the present paper.

Figures 7, 8 and 9, respectively, show a general view of Ridge A3, a cross-section of the ridge, and its salinity-temperature-brine volume profiles. The profile locations are referenced to the distance axis in Figure 8. The ridge consisted in large part of ice blocks 14 to 20 cm thick, indicating that it formed when the surrounding ice was thin. Salinities in the ridge are consistently lower than in the surrounding ice and show less variation. The temperature profiles are all roughly linear, with surface temperatures varying between -6 and -9C. The ice in the ridge, therefore, has effectively the same average temperature as the surrounding plate ice. As a result of these temperature and salinity profiles, the brine volume in the ridge was consistently lower than in the surrounding ice.

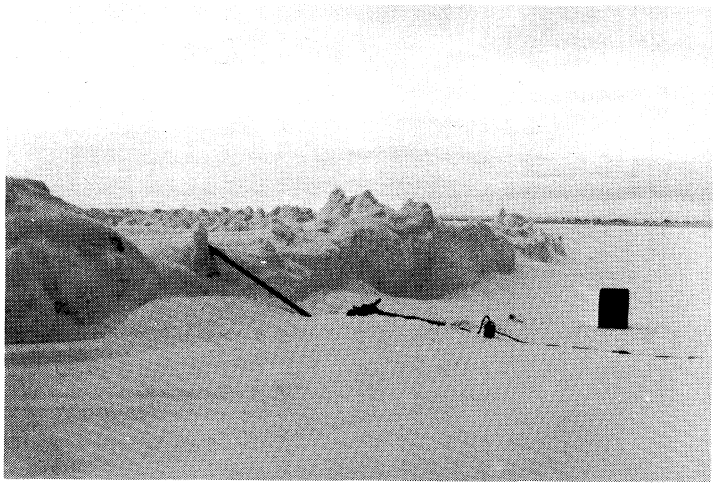

Figure 7. North edge of Ridge A3 on the profile line.

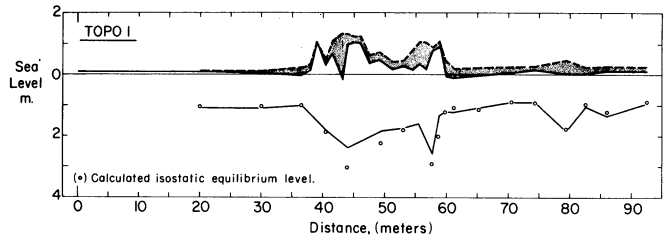

Figure 8. Transverse cross-section of Ridge A3, north of Barrow, Alaska.

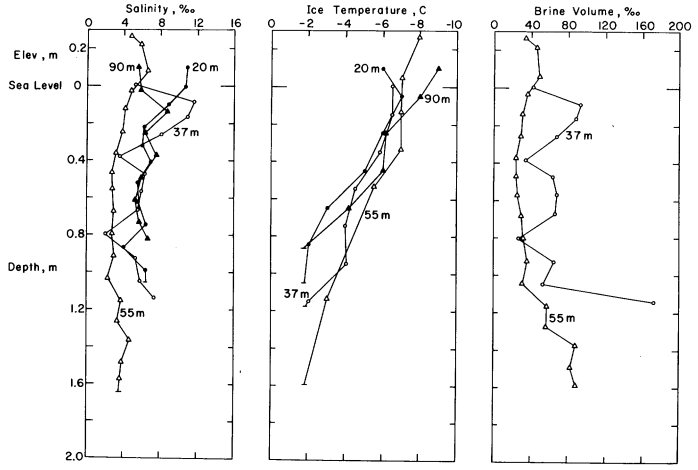

Figure 9. Salinity, temperature and brine volume profiles of Ridge A3.

No large voids were observed below the water line. The ice was surprisingly "solid" when cored and it was apparent from examining the cores that the ice in the ridge was composed of innumerable small ice blocks that had been frozen together. This type of structural identification was simplified by the fact that the plate ice incorporated within the ridge has a pronounced horizontal layering of plankton. Many times these brownish layers would be found tilted at high angles in cores from the ridges. Figure 10 is an underwater view of a portion of the keel of a smaller but similar ridge that he just formed. Note the numerous ice fragments that have been mashed together. The open circles in Figure 8 indicate the calculated isostatic levels of the lower ice surface based on the average determined densities of the snow and ice in the ridge. The sheet surrounding the ridge is in isostatic equilibrium. However, the ice in the ridge itself does not appear to be isostatically compensated. This is also indicated by the deflections in the plate ice at the edge of the ridge where flooding was observed after coring.

The significantly larger snow accumulation on and around the ridge indicates that the ridge acted as a snow fence. The fact that ridges are natural barriers to drifting snow is immediately apparent to anyone who has flow over the arctic pack in the winter.

Figure 11 shows the cross-section profile of ridge (A7). Detailed sonar observations on both the maximum keel depth and the keel shape of this as well as other ridges proved to be in very good agreement with the results of direct drilling. A general view of this ridge is presented in Figure 12. Examination of the ice blocks in the ridge showed that there were two principal thicknesses: 15 to 20 cm and 50 to 60 cm, indicating that the ridge had either been active at two different times or had formed by the interaction of ice sheets of two different thicknesses. The coring logs, temperature and salinity profiles and calculated

Figure 10. Underwater photograph of the ice in Ridge A1. The light area in the upper left-hand corner is the lower surface of the undeformed plate ice.

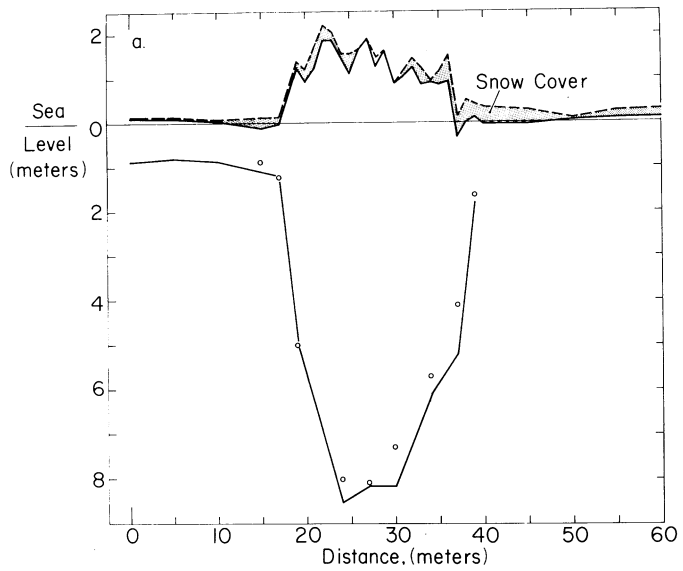

Figure 11. Cross-section of Ridge A7.

Figure 12. Drilling on Ridge A7.

brine volume profiles are shown in Figure 13. As indicated in the core logs, this ridge was heterogeneous in structure with "layers" of sea ice alternating with snow and granular slush ice. The slush ice was distinctive with an equiaxed structure and a grain size of 1 to 3 mm. Because the slush was very poorly bonded, core recovery was poor. Pronounced deterioration cavities up to 2 cm in diameter were observed in the lower portion of the ridge.

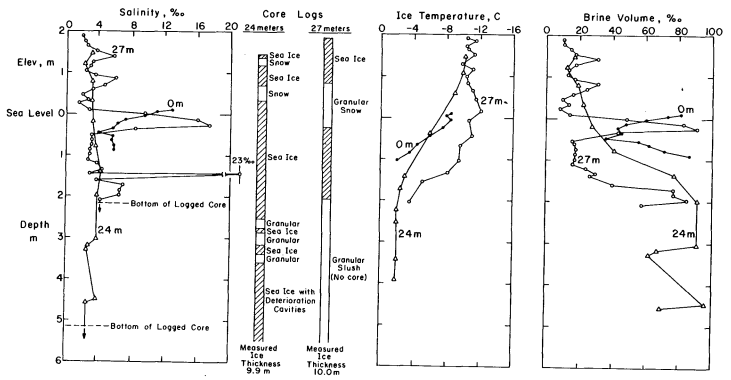

Figure 13. Salinity, temperature and brine volume profiles from Ridge A7.

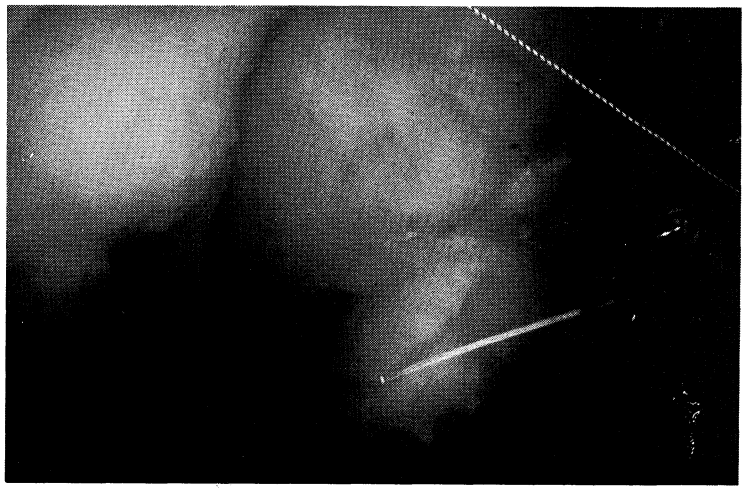

Figure 14. Underwater photograph of the keel of Ridge A7.

Figure 14 is an underwater photograph of a portion of the ridge keel. Note the rounding of the corners of the larger blocks, indicating that appreciable melting has occurred, and the general deteriorated appearance of the ice. In this ridge the calculated isostatic levels are of doubtful value because of difficulties in obtaining adequate densities for the snow and slush. However, the deflections of the plate ice near the ridge suggest that the weight of the ridge is again partially supported by the surrounding ice sheet. The ice temperatures are as expected: the surface of the ridge is colder than the surface of the surrounding plate ice and the keel of the ridge is very near the freezing temperature of the sea water. With the exception of two "irregularities", the salinities of the ridge ice averaged $4^0/_{00}$.

Figure 15 shows the cross-sectional profile of a large grounded ridge located some 10 km southwest of Lost River on the Seward Peninsula (Kovacs, 1971). A ground view of the ridge is presented in Figure 16. The ridge had formed only a few days earlier as the result of storm winds from the south. The largest blocks in the ridge were 1.6 m thick which is comparable with the thickest undeformed

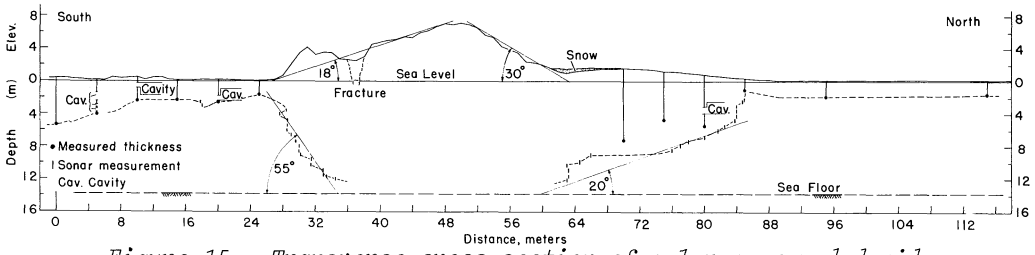

Figure 15. Transverse cross-section of a large grounded ridge approximately 10 km southwest of Lost River, Alaska.

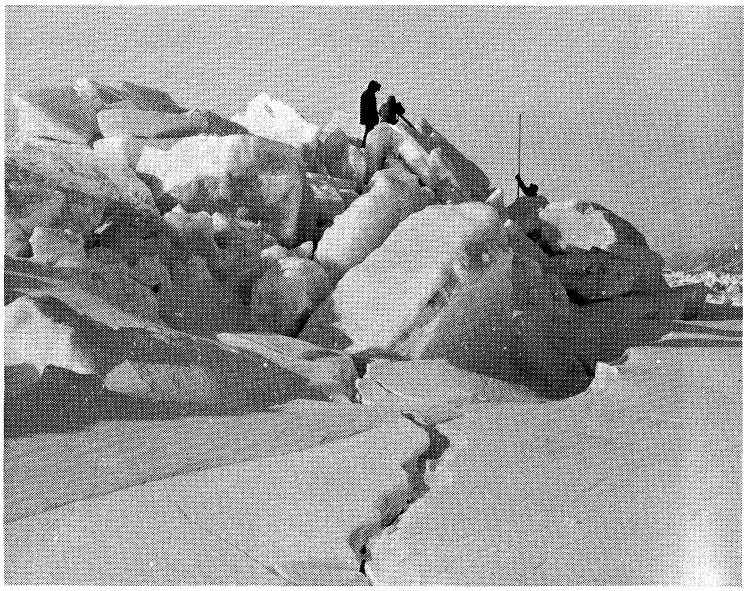

Figure 16. North face of the grounded ridge shown in Figure 15. Note the variation in thickness of the incorporated ice blocks.

plate ice in the area. Large amounts of thinner ice were found to occur in quite unstable positions and great caution had to be exercised while walking on the ridge. The poor bonding in the upper part of the ridge is probably related to the low temperatures that existed (-20 to -40C) during the short life of the ridge. That this ridge had undergone a gradual downward isostatic readjustment since its formation, could be ascertained by examining the layered ice that formed in cracks alongside the ridge and the nature of the flooding of the surrounding plate-ice. Note in Figure 15 the number of cavities observed in the sea ice during the drilling process.

A cross-section of a multi-year ridge from the Beaufort Sea is shown in Figure 17. An aerial view of the ridge is given in Figure 18. The subsurface portion of the ridge is significantly larger than the above-water portion. Exploratory coring revealed no cavities and the ice appeared to be sound, as indicated by augering resistance.

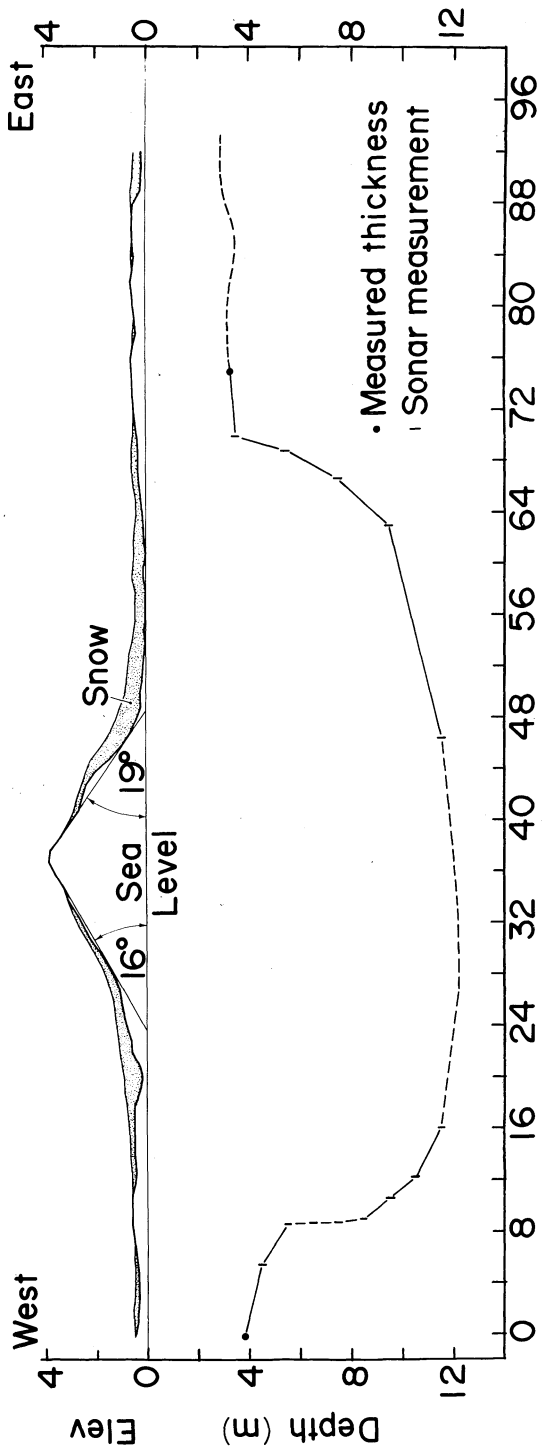

Figure 17. Cross-section of a multi-year ridge.

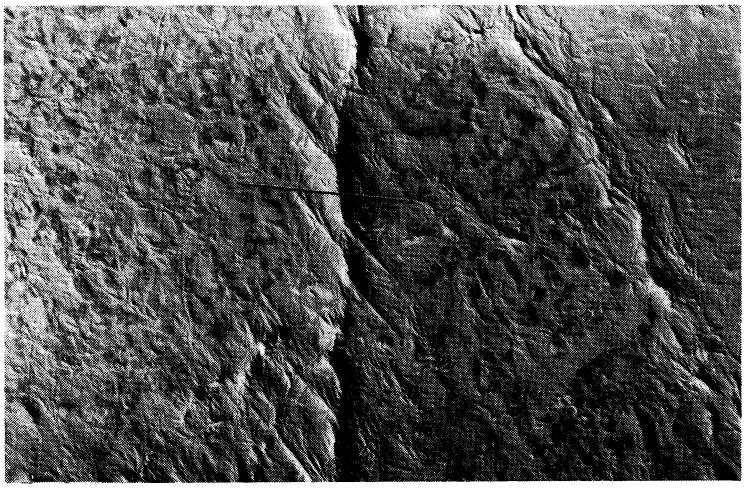

Figure 18. Aerial view of multi-year ridge (center of photo) and the undulating terrain of the surrounding multi-year floe. White line indicates position of the cross-section shown in Figure 17.

The salinity, temperature and brine volume distribution of the ice at the center of the ridge, is shown in Figure 19. The ice near the surface of the ridge was found to be bubbly indicating that the brine pockets had drained, thereby "freshening" the ice. This is born out by Figure 19 which shows the salinity of the ice to be virtually zero at the surface but increasingly gradually with depth to about $4^{0}/_{00}$ at the bottom.

The fact that pressure ridges act as snow fences is again clearly illustrated in Figure 17. Here it is seen that the greatest snow accumulation occurred along the toe of the sail where it was in excess of one meter thick.

The cross-section profile shows that the surface of the ice approaching the ridge sail is deflected downward. The deflection is believed to be partly related to snow loading and partly related to a reduction in buoyancy, as a result of keel ablation. Both effects would cause the ridge to subside in the process of seeking isostatic equilibrium.

The internal structure of a multi-year ridge which has split apart is shown in Figure 20. The distribution and size of the ice blocks incorporated into this ridge and the refrozen water between the blocks are clearly shown. The lack of voids between the blocks is very apparent. Note also the dark plankton band within the largest ice block. There is little doubt from our studies that multi-year ridges are structurally sound and would pose a severe threat to improperly designed off-shore structures.

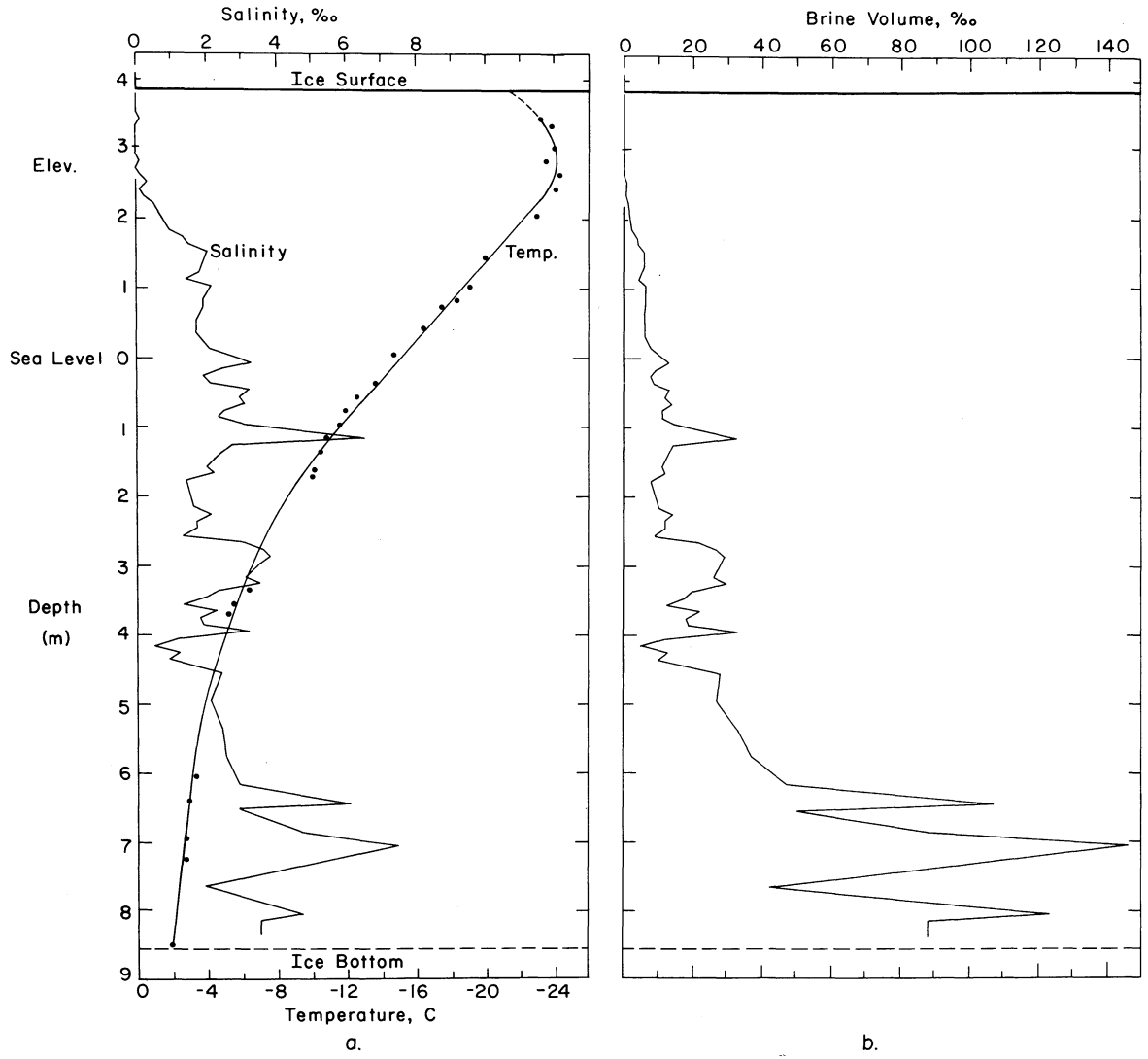

Figure 19. Salinity, temperature and brine-volume profiles of the ice at Station 37 on the cross-section shown in Figure 17.

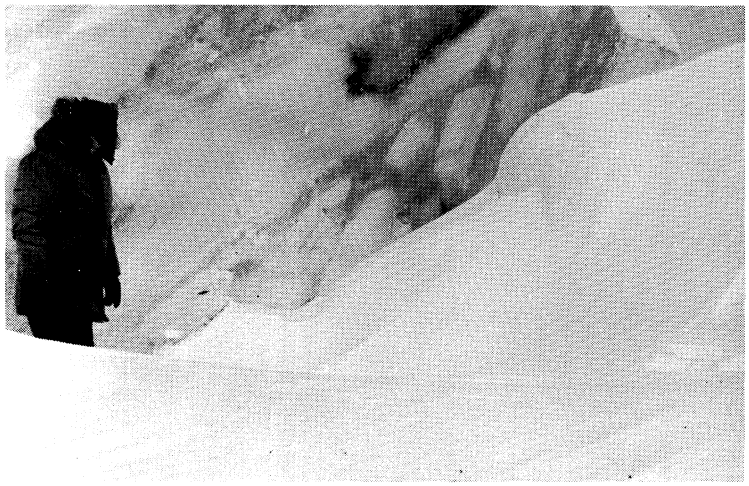

Figure 20. Internal structure of a multi-year pressure ridge which has split.

DISTRIBUTION

Characterizing the distribution of ridging in time and space over the Arctic Ocean is, of course, very difficult. New ridges are continuously being generated and once formed drift laterally with the general motion of the pack. Also it is known that brine drainage, sublimation and melting will, during the spring and summer, cause significant changes in the geometry and properties of the upper portions of ridges. It is quite possible that a similar modification of the geometry of ridge keels occurs through the year although information on this subject is almost nonexistent. Nevertheless, it is possible, based on information obtained during the BIRDSEYE flights, to separate the Arctic Ocean into at least three ice provinces (Wittmann, personal communication):

1. A *Coastal Province* consisting of a zone of shore-fast ice bordered by a flaw zone of disturbed ice and in some locations a recurring flaw lead.

2. An *Offshore Province* mainly composed of relatively unstable first-year ice which has usually experienced a considerable amount of deformation.

3. A *Central Arctic Basin Province*, which is by far the largest province of the three and is primarily composed of multi-year ice. The amount of deformation in this province is commonly thought to be less than in areas closer to shore.

All these Provinces can undoubtedly be further sub-divided as more information becomes available. For instance in the Central Arctic Basin Province the surface topography of the ice in the transpolar drift stream appears to be significantly rougher (angular ridges and hummocks) than the topography of the ice in the Pacific Gyral (gentle rounded hummocks) (Koerner, 1970).

Coastal Province

The Coastal Province is of great interest to the present symposium because it primarily encompasses areas of shallow water (<20 m) where under-ice submarine and construction operations are difficult. Pipe lines and drill heads can, of course, be installed under the fast ice through holes cut or blasted in the ice. In the summer the Coastal Province is usually relatively ice free allowing for the undertaking of construction operations similar to those in areas with more temperate climates.

Offshore Province

The Offshore Province is also of interest because it lies over the Continental Shelf with water depths commonly under 100 m. With such water depths, pressure ridge avoidance is an important consideration in submarine tanker operations and the distribution of ridge keels would also be important in estimating the optimum distribution and size of sea floor installations. The width of the Offshore Province is quite variable because the multi-year pack north of the province often moves southward, replacing much of the ice of this zone. We will consider the province width to be roughly 200 nm. In the winter the province contains a large amount of first-year ice of a thickness equal to or less than that of the undeformed fast ice off the coast. As shown in Figure 21, which is based on data from the BIRDSEYE flights, ridging in this area is quite intense. Figure 22 shows a representative aerial view of ice from this province taken north of Barrow. The infor-

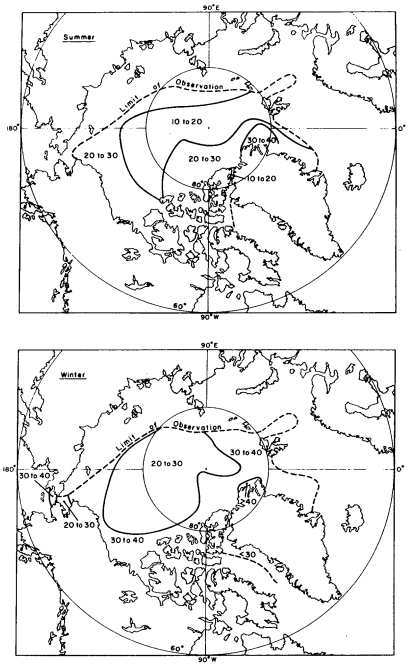

Figure 21. Maps of ridges per nautical mile during the winter and during the summer as observed by the Birdseye flights (Wittmann and Schule, 1966). The dotted line indicates the areal extent of the data.

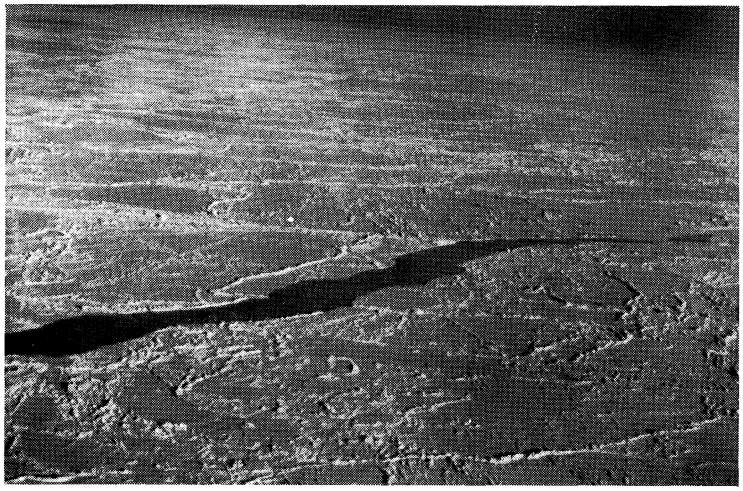

Figure 22. Ridging in the Offshore Province north of Barrow, Alaska.

mation available on the ice conditions in this province is summarized in Table I. According to the BIRDSEYE results, 26% of the province area contains either hummocks or ridges in the winter. Similar results have been obtained from sonar profiles which have occasionally reported zones several hundred kilometers wide that were more than 50% covered by hummocked ice.

Table I. Ice conditions in the Offshore Province.

Source	*Subject*		*Season* *Winter*	*Summer*
BIRDSEYE	Concentration (areal, %)	average	99	78
		range	70-100	8-100
	Ice types (areal, %)	young	7	5
		winter	46	46
		multi-year	46	27
	Topography (areal, %)	large ridges and hummocks (>3 m high)	21	15
		small ridges and hummocks (<3 m high)	5	8
	Number of water openings	>30 m/100 nm	34	76
		<30 m/100 nm	134	73
Submarine	Topography (linear, %)	openings	2	9
		ice	98	91
		keels	12	7

Figure 23 shows the frequency distribution of ridge heights as well as the number of ridges per nautical mile in both the Chukchi and Beaufort Seas which are part of the Offshore Province. The results agree with recent winter observations from northern Baffin Bay which indicate that in first-year ice, ridges sails

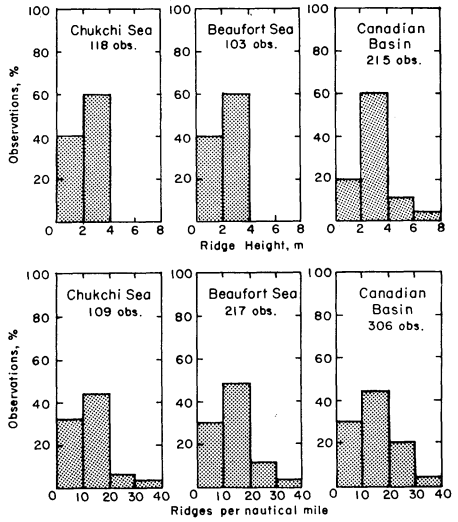

Figure 23. Winter distributions of ridge heights and the number of ridges per nautical mile for the Chukchi and Beaufort Seas (Offshore Province) and the Canadian Basin (Central Arctic Basin Province). The data is from the Birdseye flights (Wittmann and Schule, 1966).

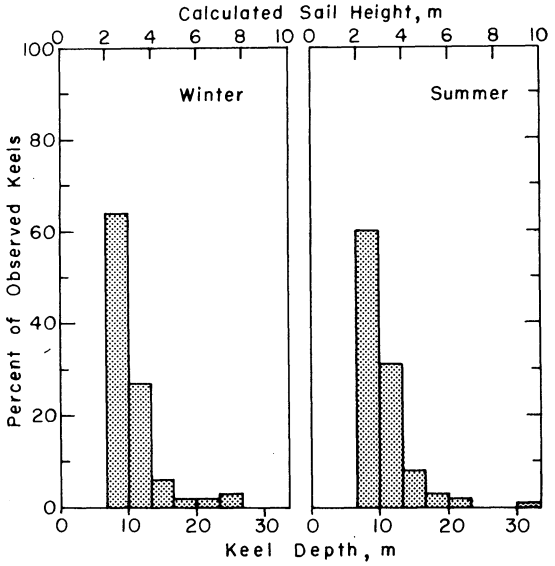

Figure 24. Percentage of keels of different drafts in the Offshore Province as observed by sonar on the Sargo and Seadragon cruises. Track lengths are 35 (winter) and 54 (summer) nm. The sail heights are calculated assuming a keel to sail height ratio of 3.3 to 1.

exceeding 4 m in height are not common. The percentage of keels of different depths as observed by the Sargo and Seadragon cruises is shown in Figure 24. The sail heights are calculated assuming a keel/sail ratio of 3.3/1. This ratio is based on the Makarov-Wittmann pressure ridge model (Wittmann and Schule, 1966) and may be somewhat low for first-year pressure ridges (Kovacs 1971) although it does appear to satisfy the ratio for multi-year ridges (Kovacs, et al. 1971). However, surface observations of ridge heights by several expeditions operating in the Arctic Basin indicate that a maximum non-grounded ridge height of 13 m is reasonable.

As mentioned earlier, a feature observed in all parts of the pack, but particularly common in the first-year ice of the Offshore Province, is the hummock field. In these fields essentially all the ice is broken and distributed in an apparently chaotic fashion. Figure 25 shows a surface view of a hummock field north of Barrow. The frequency distribution of sail and keel elevations in these field is presumably similar to the distribution of sail and keel elevations in normal ridges. There are no detailed studies of the sizes of such fields but our observations indicate that some of them have lateral dimensions of several kilometers. A view of a very severely hummocked area in the Chukchi Sea are shown in Figure 26. The hummocks in this field reached heights of 7 m and were effectively continuous.

Figure 25. View of a hummock field north of Barrow, Alaska.

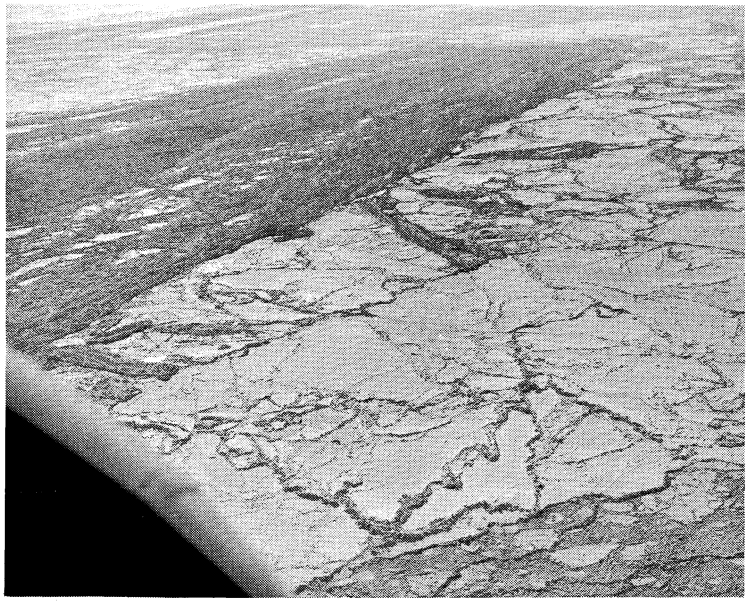

Figure 26. View of a rectangular hummock field observed at the Arctic Circle in the Chukchi Sea north of the Bering Strait. The ridges in the field reached heights of up to 7 m.

A good impression of the variation in surface relief in this province in the winter can be obtained by examining the laser profiles shown in Figure 27. They were taken by NAVOCEANO on 17 April 1970 from approximately 60 nm north of Prudhoe Bay. The ice is very rough with several ridge heights between 4 and 5 m. The ice here is predominantly first-year. The long period elevation changes are the result of aircraft motion.

During the summer the ice conditions in the Offshore Province are extremely variable, with the location of the pack boundary ranging from near-shore to up to 200 nm offshore. Table I summarizes observations in the ice covered portions of the province. As can be seen by comparing Figure 28 with Figure 23, there is a slight decrease in ridge heights, presumably due to melting. There is also a marked decrease in the number of ridges per nautical mile. This is probably caused by the melting and collapse of a number of ridges in the more highly deformed areas. A similar trend is suggested by the sonar results shown in Figure 24.

In order to determine possible ridge periodicities an analysis of the power spectrum of the bottom surface of pack ice has been made by Hibler and LeSchack (1971) based on under-ice sonar records from the Beaufort Sea. The power spectra and the frequency distribution of ice thickness, along a straight 13.3 km track is shown in Figure 29. The power spectra of some of the profiles indicate marked

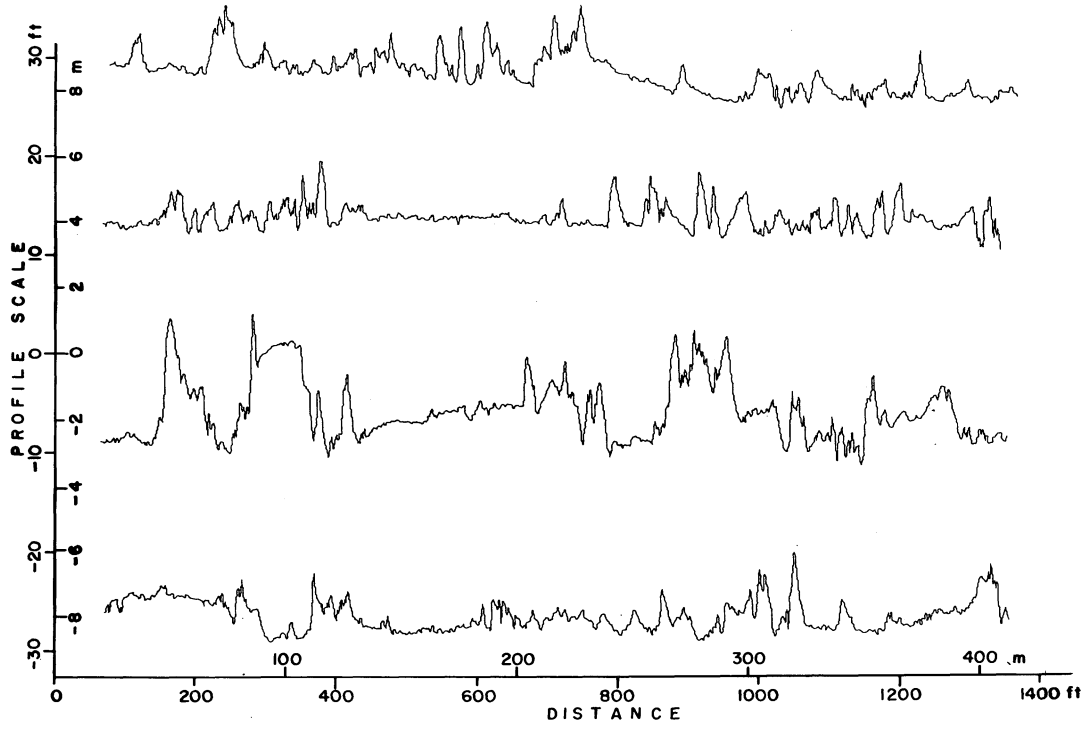

Figure 27. A laser profilometer track taken on 17 April 1970 roughly 60 nm north of Prudhoe Bay, Alaska. The run heading is 348°: the profile runs consecutively from upper left to lower right. The zero location of the profile scale is arbitrary.

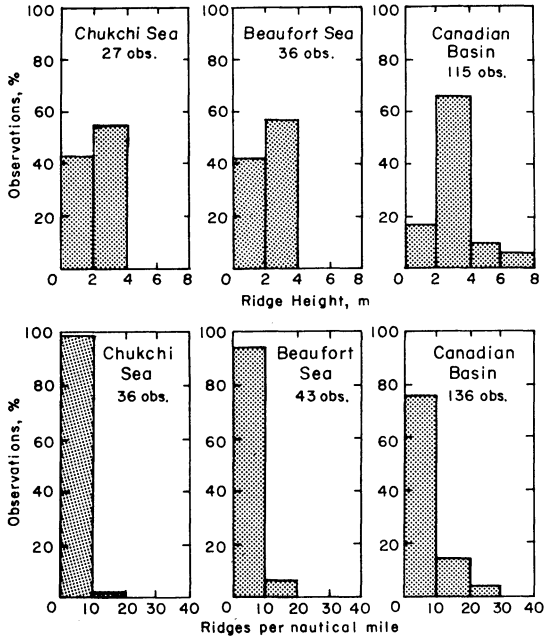

Figure 28. Summer frequency distributions of ridge heights and the number of ridges per nautical mile for the Chukchi and Beaufort Seas (Offshore Province) and the Canadian Basin (Central Arctic Basin Province).

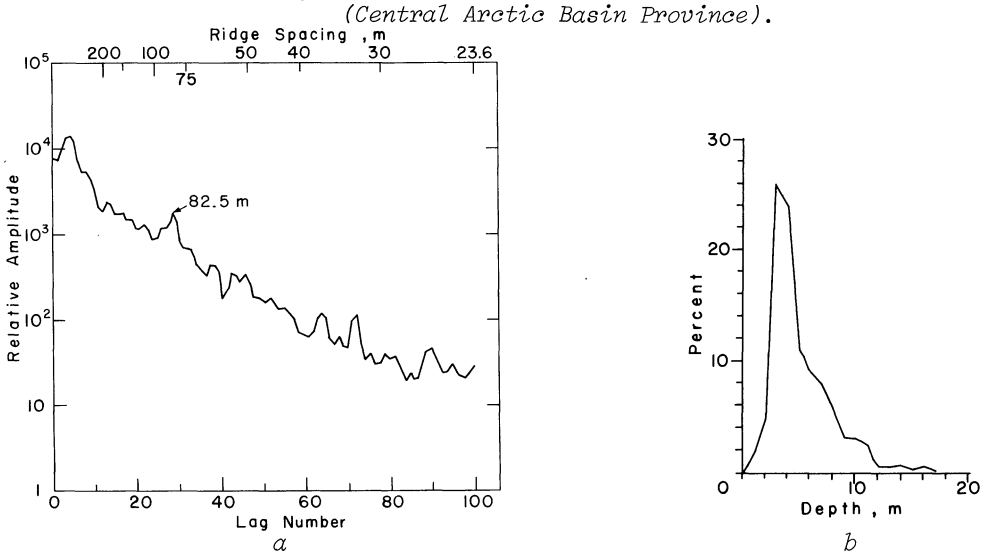

Figure 29. Power spectra of an under-ice profile in the Beaufort Sea (a) and a plot of the frequency distribution of keel depths (b) from the same profile.

peaks at some spacings (note the 82.5 m peak in Figure 29). The physical reasons for this apparent periodicity are, however, not presently understood. By comparing the power spectra from intersecting sonar tracks, Hibler and LeSchack also suggest that there is some preferred orientation in the ridge system they studied. Similar conclusions have been reached by Mock and Hartwell (1972) from a study of ridge patterns in the Beaufort Sea 30 nm east of Barrow. The Beaufort Sea study also showed that if the ridge frequency N is known ($N = n/l$ where n is the number of ridges crossed in a traverse length l), then the ridge density R_D, the total

length of the ridges per unit area, can be calculated from the simple relation $R_D = 1.57\ N$. Hibler and LeSchack have also studied the power spectra of the upper surface of pack ice using laser profiles. The results indicate that first-year ice has a greater percentage of high frequency spectral components than multi-year ice: presumably due to the weathering and smoothing of the older ice. Similar differences would be expected in the bottom roughness.

Central Arctic Basin Province

In the northern portion of the Offshore Province, there is a gradual increase in the amount of multi-year ice until the consolidated multi-year floes become the dominant aspect of the terrain. This marks the edge of the Central Arctic Basin Province which extends the remaining distance to the North Pole. This Province is of less interest to this Symposium because of the very deep water under the ice. However, because of the very large portion of the surface of the Arctic Ocean that would be designated as part of this Province, a brief summary of the ice conditions are given here (Table II). The frequency distribution of ridge heights as well as the number of ridges/nm for the Canadian Basin is given in Figure 23 as observed by the BIRDSEYE flights. Note that although it is commonly stated that there is less ridging in the central portion of the Arctic Ocean than nearer shore (see for example Figure 21), the data in Figure 23 do not indicate any major difference. Also, both the BIRDSEYE data and the submarine data summarized in Figure 30 indicate an increase in the number of large ridges in the Central Arctic Basin Province relative to the Offshore Province. Most of the ridges in the Central Arctic Basin Province are composed of the thinner first-year ice and should be similar to the ridges in the Offshore Province. Five percent of the ridges, however, contain appreciable amounts of multi-year ice. These probably comprise the larger ridges.

Histograms of sea ice drafts in the Central Arctic Basin Province as determined by sonar are given in Figure 31. Pressured ice with drafts greater than 6.7 m is not included here. Based on other experience in the Arctic Ocean, 2.5 to 3.5 m can be taken as a representative thickness for undeformed multi-year ice. The undeformed first-year ice can, or course, be any thickness less than 2.3 m depending upon its date of initial formation.

Figure 32 shows a laser profilometer trace of multi-year ice in the Central Polar Basin. There is a general decrease in surface relief relative to the laser profile from the Offshore Province (Figure 27). Note the undulating topography of the old floes.

The summer ice conditions in this Province are also summarized in Table II. The average area of open water increases to between 5 and 8%. There is also a sharp drop in the number of ridges per nautical mile. The BIRDSEYE data do not indicate a pronounced change in the distribution of ridge heights. The sonar data (Figure 28), on the other hand, show no summer keels larger than 23 m compared with winter keels over 30 m.

Table II. Ice conditions in the Central Arctic Basin Province.

Source	*Subject*		*Season* *Winter*	*Summer*
BIRDSEYE	Concentration (areal, %)	average	99	92
		range	98-100	30-100
	Ice types (areal, %)	young	1	4
		winter	17	27
		multi-year	81	61
	Topography (areal, %)	large ridges and hummocks (>3 m high)	21	23
		small ridges and hummocks (<3 m high)	4	4
	Number of water openings	>30 m/100 nm	23	39
		<30 m/100 nm	33	53
Submarine	Topography (linear, %)	openings	1	5
		ice	99	95
		keels	15	15

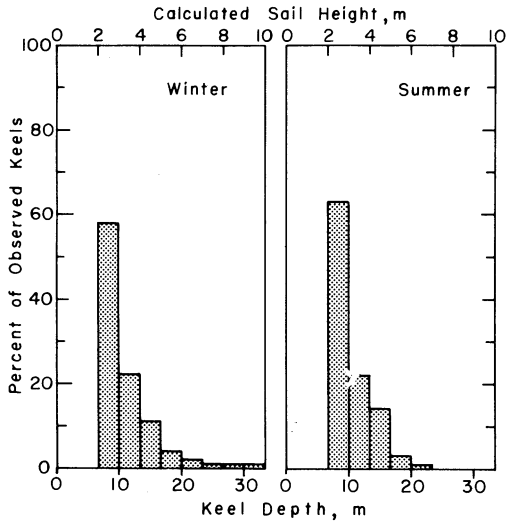

Figure 30. Percentage of keels of different drafts in the Central Arctic Basin Province as observed by sonar on the Sargo and Seadragon cruises. Track lengths are 150 (winter) and 94 (summer) nm. The sail heights are calculated assuming a keel to sail height ratio of 3.3 to 1.

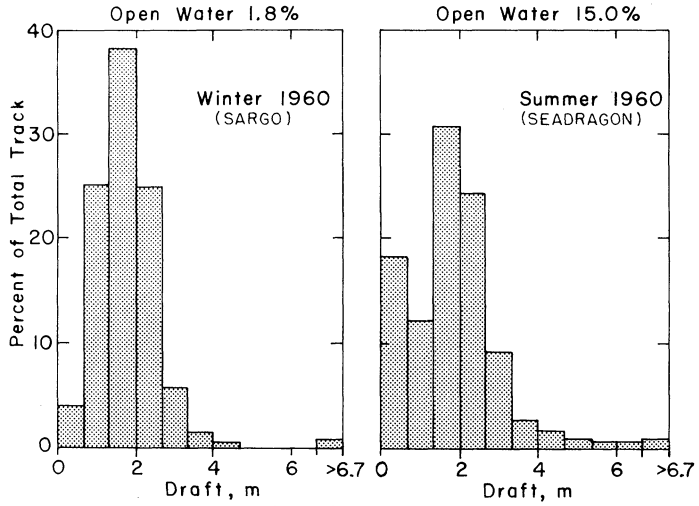

Figure 31. Histograms of sea ice drafts in the Canadian Basin; pressured ice with drafts greater than 6.7 m is excluded (data from Wittmann and Schule, 1966).

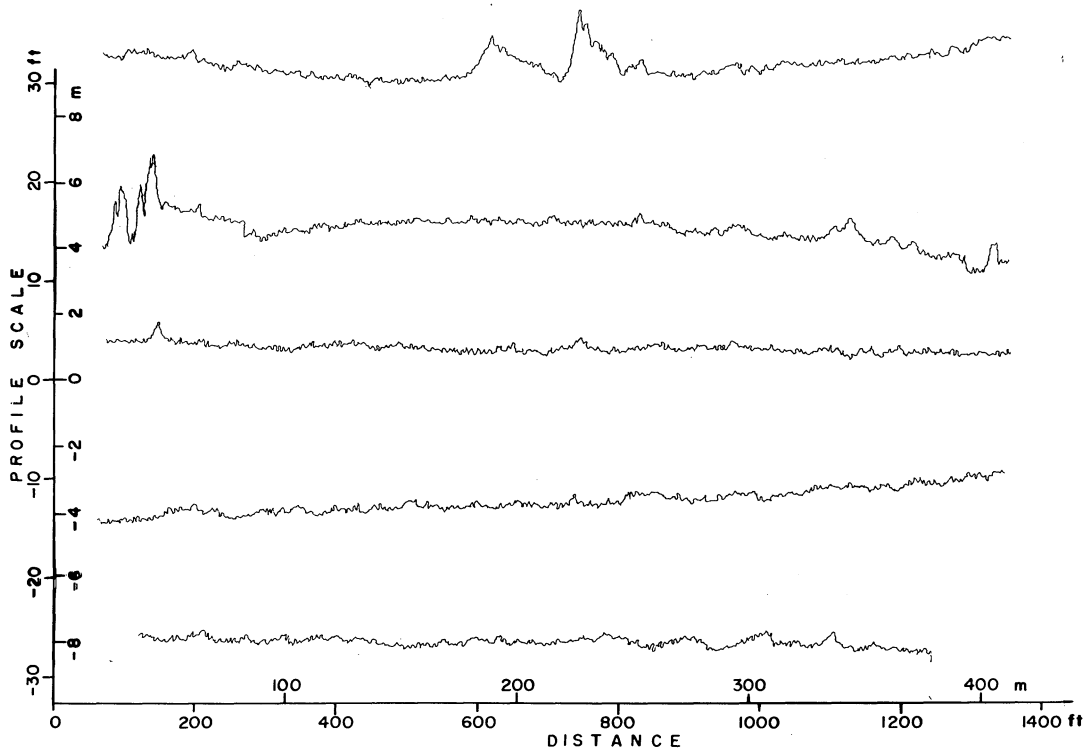

Figure 32. A laser profilometer trace of multi-year ice in the Central Polar Basin. The aircraft motion has not been removed. The profiles run consecutively from upper left to lower right. The zero location of the profile scale is arbitrary.

STATISTICAL ASPECTS OF PRESSURE RIDGES

In the preceding sections we have discussed observed variations in ridge distributions from region to region. Here we will discuss the particular problem of the ratio of deeper ridges to shallower ridges for a given area as well as the average spacing between ridges. This will then be applied to predicting the number of impacts of large ridges upon offshore structures. By assuming the randomness of different ensembles of ridges Hibler, Weeks and Mock (1971) have constructed a theoretical ridge distribution model which is found to be in excellent agreement when tested against observed ridge depth distributions. For the distribution of distance between ridges, the above authors also find that to a good approximation ridge position may be assumed to be random. This yields a negative exponential distribution for the between ridge spacing distribution.

The basic results for the ridge depth distribution may be summarized as follows. One first considers the ensemble of all collections of ridges that yield the same amount of ice deformation in a given area. The total number of arrangements of ridges having n_i ridges in a given depth interval is in general given by the multinomial expansion. Assuming all possible arrangements are equally probable subject to the constraint of constant deformation, a variation calculation is carried out. This yields, with the assumption that the ridge cross sectional area is given by $A_i = \lambda h_i^2$, the following normalized probability density for ridges greater than 6 m.

$$P(h)\,dh = 2\sqrt{\frac{\lambda}{\pi}}\;\frac{e^{-\lambda h^2}\,dh}{[1 - \mathrm{erf}\,(\sqrt{\lambda}\,6)]} \qquad (1)$$

Here $P(h)\,dh$ is the probability that a given ridge (over 6 m deep) will have a depth between h and $h + dh$. The parameter λ is determined from the average ridge depth by solving a simple integral equation. It should be pointed out that care should be taken when using this formula because it has been assumed that the cross sectional area of a ridge is a constant times the ridge depth squared. This is perhaps reasonable for deep ridges but for smaller ridges the constant may well vary with depth (i.e., the ridge slope angle may change.)

Test of this theoretical distribution versus experimental data in general shows excellent agreement. Typical values of λ range from 0.014 m^{-2} for areas of medium ridging intensity to 0.007 m^{-2} for areas of high ridging intensity. For an area with similar morphology λ appears to be relatively independent of the ridging density - i.e. this suggests that the characteristic probability density may well apply to large regions independent of the density of the ridging. Figure 33 shows the average percentage distribution taken from 49 sets of ridge distribution determined in areas of moderate ridging. As can be seen the theoretical curve fitted using only the parameter λ, fits the data, the average ridge spacing was found to be 244 m with a standard deviation of 30 m.

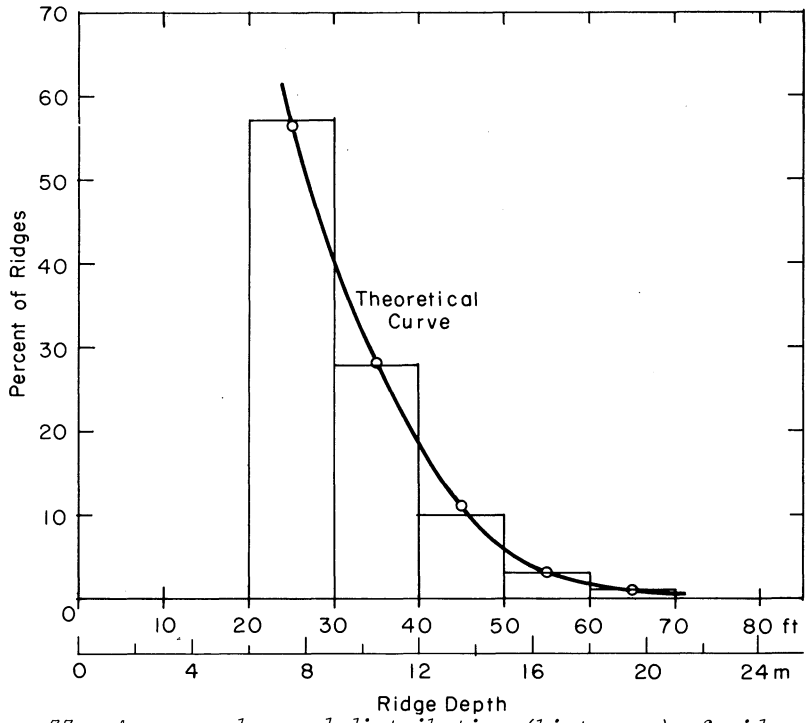

Figure 33. Average observed distribution (histogram) of ridges deeper than 20 ft. from USN Sargo sonar records over a distance of approximately 150,000 yards, and best fit of theoretical distribution. The theoretical curve was fitten by only using the mean ridge depth so it is a one parameter fit.

SURVIVAL OR IMPACT PROBABILITY

Using the depth distribution discussed in Eq. 1, it is possible to estimate the survival time of an object placed at a given depth below a moving ice sheet. The same general approach could also be used to compute the expected number of collisions equal to or greater than a given magnitude in a specified length of time on al off-shore structure. First we need to know the total number of ridges with drafts greater than Q per nautical mile. Using equation 1 for the depth distribution this number is given by:

$$N_0 = N_1 \int_Q^\infty P(h)\, dh = N_1 \frac{[1 - \text{erf}\ (\sqrt{\lambda}\, Q)]}{[1 - \text{erf}\ (\sqrt{\lambda}\, 6)]} \qquad (2)$$

Here N_1 is the total number of ridges with a depth greater than 6 m per nautical mile which we will take to be 10. As a value of λ for further calculations we take $\lambda = 0.014\ m^{-2}$, a reasonable value for moderately ridged ice.

Now suppose that we place an object of arbitrary width d beneath the ice pack, at depth Q. We can, therefore, consider the ice pack moving over an object at a speed r for a time t as rt/d random samples of length d of the subsurface profile. Because the probability of finding a ridge with a keel greater than Q in a given length d is small and we are assuming random sampling, the probability can be

considered to obey a Poisson distribution

$$P\ (n) \ = \ \frac{[N\ d\ N_0]^n}{n!} \quad \exp\ [-d\ N_0\ N] \tag{3}$$

where $P\ (n)$ is the probability of finding n ridges with keels greater than Q in N random samples of length d. Note that $N = rt/d$ so that $P\ (n)$ is independent of d. We only introduce d as a device for deriving the distribution.

Using the above distribution, the probability of the object not being touched (survival probability) by the ice after time t is

$$W\ (t) \ = \ \exp\ [-N_0\ rt] \tag{4}$$

which yields an average value of t of $\gamma = 1/N_0 r$ which we call the lifetime. A plot of γ as a function of the depth Q is given in Fig. 34.

The basic assumption made in deriving the Poisson distribution was that an object moving under an ice cover samples regions of ice randomly. Since we have placed the object at random to begin with, the assumption of random sampling up to the 1st collision at least should be quite valid. However, in general, as we move along a profile of sea ice if there are periodicities in the ridge structure this assumption will not be completely valid. Power spectra analysis by Hibler and LeSchack on limited tracks of under ice profiles did indicate certain periodicities but it should be emphasized that the deviation of the spectral peak from the smooth spectrum was small relative to the total spectrum at the peak frequency. In other words the periodicity is essentially a perturbation on the randomness and we would still expect that adjacent lengths along a profile have equal probability of ridge occurrences and thus the Poisson distribution should hold spatially, i.e. the probability of finding n ridges in a profile length L is

$$P\ (u) \ = \ \frac{(L\ \mu)^n}{n!}\ e^{-L\mu} \tag{5}$$

where μ is the average number or ridges per unit length. This assumption has been tested at some length by Hibler, Weeks and Mock (1971) with good agreement.

Another relevant point that should be made here is that if the Poisson distribution is obeyed then it follows mathematically that the probability density for spacings between adjacent ridges is also a negative exponential, i.e.:

$$P\ (x)\ dx \ = \ \mu e^{-\mu x}\ dx \tag{6}$$

where $P\ (x)\ dx$ is the probability of two adjacent ridges being separated by a distance between x and $x + dx$. Observed distributions of ridge spacings are often exponential which further substantiates the random nature of the ridges.

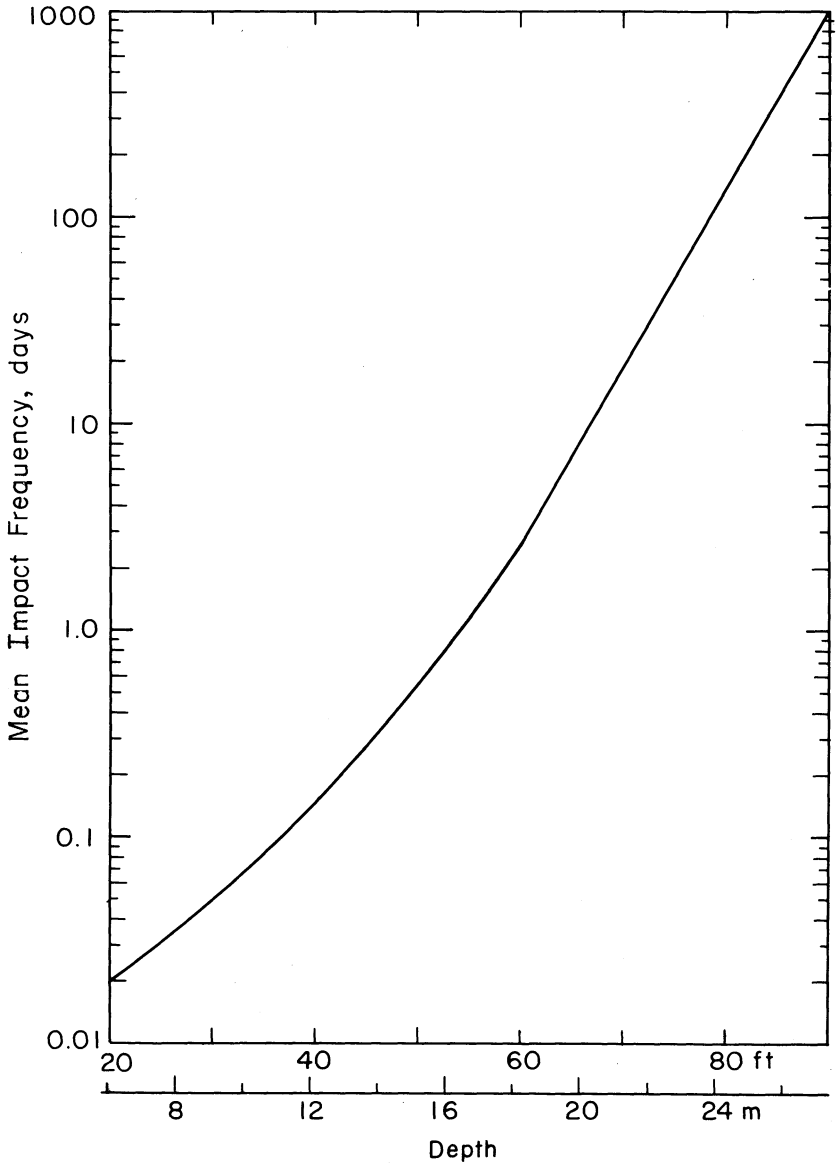

Figure 34. The mean lifetime of an object as a function of depth, Q, of the object below the water surface. The ice was assumed to be moving over the object at a velocity of 5 nm/day and an average of 10 ridges over 6 m deep per nautical mile were assumed. Since the lifetime scales inversely with the average number or ridges and the velocity, the figure may also be used to estimate lifetimes for any velocity and ridge density.

With respect to the calculation of survival times or impact probabilities, the important point is, that given the validity of equations (1) and (5), it is only necessary to determine the mean ridge depth and the average number of ridges per unit length. These quantities can easily be measured by sonar from a moving submarine or by laser from a moving airplane.

CONCLUSION

Our observations on the geometry and structure of ridges may be summarized as follows:

1. The degree of bonding between ice blocks and, therefore, the overall structural integrity of first-year ridge keels appears to be variable, changing with the age of the ridge and presumably the initial temperature of ice being incorporated into the ridge. It can be shown that during the winter the cold reserve of ice blocks being incorporated into a ridge keel can be sufficient to cause significant inter-block ice growth.

2. Lack of local isostatic adjustment is common in ridges. In new ridges a significant portion of the load of the ridge is supported by deflections in the surrounding plate ice. When ridges form by thrusting, their upper and lower portions may be laterally separated by tens of meters. This obviously results in a non-isostatic condition which is compensated by deflections of the local plate ice. With multi-year ridges the effects of snow loading and keel ablation cause a gradual subsidence of the ridge and deflection of the surrounding plate ice.

3. A representative salinity for the ice in first-year ridges we examined was $4^0/_{00}$ and $3^0/_{00}$ for multi-year ridges. The temperature profiles were reasonably linear except in the lower parts of ridges with pronounced keels where temperatures were roughly constant at near freezing values.

4. Present results do not support the contention that the average surface slope angle in the above-water portion of a first-year ridge (25°) is larger than that in the underwater portion (32°).

5. Ridges act as effective snow fences, causing large amounts of snow to accumulate both in and around their upper parts.

6. Multi-year ridges appear to be massive in size and "solid" giving little doubt that they represent formidable obstructions for ships to penetrate and for offshore structures to resist when under way.

7. It appears doubtful that the cross-section profiles of all ridges can adequately be represented by any one geometric model. We, however, feel that once ridges are separated into classes based on the mechanics of their formation, a given geometric model may well apply to the whole class.

8. Based upon a theoretical ridge depth distribution "survival times" or impact probabilities with ridges of a given size may be calculated in a straightforeward manner from a knowledge of the mean ridge depth and the number of ridges per unit length.

ACKNOWLEDGMENTS

The field work reported in this paper was performed by the authors in conjunction with G. Frankenstein, N. Smith and S. Ackley of CRREL, L. Breslau, P. Welsh, Lt. Trammel and LCDR J. McIntosh of the U.S. Coast Guard and W.J. Campbell of the U.S. Geological Survey. Their assistance is gratefully acknowledged. The logistic support of the Arctic Research Laboratory, the AIDJEX Project and the Canadian Polar Continental Shelf Project is appreciated. The overall pressure ridge research project was funded by the U.S. Coast Guard and the Advance Research Projects Agency.

REFERENCES

Dunbar, M. and W. Wittman (1963) Some features of ice movement in the Arctic Basin In *"Proceedings Arctic Basin Symposium, 1962"*. Arctic Institute of North America, p. 90-108.

Herbert, W. (1970) The first surface crossing of the Arctic Ocean. *The Geographical Journal*, Vol. 136, Part 4, p. 511-533.

Hibler, W.D. and L.A. LeSchack (1971) Power spectrum analysis of undersea and surface sea ice ridge profiles. U.S. Army Cold Regions Research and Engineering Laboratory (USA CRREL) Technical Note, 18 pp. (Submitted to the *Journal of Glaciology*).

Hibler, W.D., W.F. Weeks and S.J. Mock (1971) Statistical aspects of pressure ridge distributions. USA CRREL Technical Note (to be submitted to the *Journal of Geophysical Research*).

Koerner, R.M. (1970) Weather and ice observations of the British Trans-Arctic Expedition 1968-9. Weather, Vol. 25, No. 5, p. 218-228.

Kovacs, A. (1971) On pressured sea ice. International Sea Ice Conference, Reykjavik, 30 pp.

Kovacs, A., W.F. Weeks, S. Ackley and W. Hibler (1971) Structure of a multi-year pressure ridge (AIDJEX 1971). USA CRREL Technical Note, 22 pp. (Submitted to *Arctic*).

Mack C. (1967) Essentials of statistics for scientist and engineers. Plenium Press, New York, 174 pp.

Mock, S.J. and A.D. Hartwell (1972) Quantitative analysis of pressure ridge orientation. (Submitted to the *Journal of Glaciology*).

Weeks, W.F. and A. Kovacs (1970a) On pressure ridges. USA CRREL draft contract report to U.S. Coast Guard, 60 pp.

REFERENCES (Cont'd)

Weeks, W.F. and A. Kovacs (1970b) The morphology and physical properties of pressure ridges: Barrow, Alaska, April 1969. In *"Proceedings IAHR Symposium on Ice and Its Action on Hydraulic Structures,"* Reykjavik, Iceland, Paper 3.9, 8 pp.

Witmann, W. and J.J. Schule (1966) Comments on the mass budget of arctic pack ice. In *"Proceedings of the Symposium on the Arctic Heat Budget and Atmospheric Circulation"*. The Rand Corporation (RM-5233-NSF), p. 215-246.